

e-ISSN: 3026-1473

CROWN Journal of Dentistry and Health Research

Journal website: https://phlox.or.id/index.php/crown

In Vitro and In Vivo Efficacy of a Novel Strontium-Doped Bioactive Glass Hydrogel for Dentin-Pulp Complex Regeneration

Rinna Azrida^{1*}, Bryan Helsey², Bernadette Wilson³, Mohammad Yoshandi⁴

- ¹Department of Biomedical Sciences, Deli Tua Research and Laboratory Center, Deli Serdang, Indonesia
- ²Department of Biomolecular Science and Translational Medicine, Quezon Medical Center, Quezon, Philippines
- ³Department of Otorhinolaryngology, Skopje National Hospital, Skopje, North Macedonia
- ⁴Department of Health Sciences, Tembilahan Community Health Center, Tembilahan, Indonesia

ARTICLE INFO

Keywords:

Bioactive Glass
Dentin-Pulp Complex
Hydrogel
Regenerative Dentistry
Strontium

*Corresponding author:

Rinna Azrida

E-mail address:

rinna.azrida@bioscmed.com

All authors have reviewed and approved the final version of the manuscript.

https://doi.org/10.59345/crown.v3i1.236

ABSTRACT

Introduction: The regeneration of the dentin-pulp complex is a major challenge in vital pulp therapy. This study aimed to develop and evaluate a novel injectable hydrogel composed of strontium-doped bioactive glass (Sr-BG) in a methacrylated gelatin (GelMA) matrix to promote dentin-pulp complex regeneration. Strontium was added for its dual therapeutic effects of enhancing odontogenic differentiation and inhibiting bacterial activity. Methods: We synthesized Sr-BG nanoparticles using a sol-gel method and characterized them with X-ray diffraction (XRD), Fouriertransform infrared spectroscopy (FTIR), and scanning electron microscopy (SEM). The nanoparticles were then incorporated into a GelMA hydrogel. We assessed the material's physical properties, including its swelling ratio, degradation rate, and ion release profiles (Si, Ca, P, Sr). We also evaluated its in vitro biocompatibility and odontogenic potential using human dental pulp stem cells (hDPSCs), assessing cell viability (MTT assay), alkaline phosphatase (ALP) activity, and the expression of odontogenic markers (DSPP, DMP-1, RUNX2) via RT-qPCR. We tested its antibacterial properties against Streptococcus mutans. For the in vivo evaluation, the hydrogel was used as a pulp capping agent in the mechanically exposed molars of Wistar rats. After 4 and 8 weeks, we assessed tissue regeneration using histological analysis (H&E and Masson's trichrome staining) and micro-computed tomography (micro-CT). Results: The synthesized Sr-BG nanoparticles were amorphous with a particle size of about 80-120 nm. The Sr-BG/GelMA hydrogel exhibited controlled swelling and degradation, along with a sustained release of therapeutic ions. In vitro, the hydrogel demonstrated excellent biocompatibility and significantly upregulated ALP activity and the expression of DSPP, DMP-1, and RUNX2 in hDPSCs compared to the control group (p < 0.05). The material also showed significant antibacterial activity against S. mutans. In vivo, histological analysis revealed the formation of a thick, continuous, and well-organized tertiary dentin bridge with minimal inflammation in the Sr-BG/GelMA group at 8 weeks. Micro-CT analysis confirmed a significantly greater volume and density of newly formed mineralized tissue compared to control groups treated with calcium hydroxide. Conclusion: The novel strontium-doped bioactive glass hydrogel showed significant potential for dentin-pulp complex regeneration. Its combined osteoinductive, angiogenic, and antibacterial properties make it a promising biomaterial for advanced vital pulp therapy, offering a superior alternative to traditional pulp capping agents.

1. Introduction

The dental pulp is a highly specialized mesenchymal tissue that forms the vital core of the tooth, responsible for its formation, sensory perception, nutrition, and defense. Encased within the hard, mineralized walls of dentin, the pulp is

exceptionally vulnerable to external aggressors like deep carious lesions, traumatic injuries, and iatrogenic insults during dental procedures. When this protective dentin barrier is breached, the pulp is exposed to the microbially rich oral environment, triggering a cascade of inflammatory events that can progress from reversible pulpitis to irreversible ultimately, pulp necrosis. inflammation and, Historically, an exposed pulp was often managed by complete removal through pulpectomy subsequent root canal treatment. While effective in eliminating infection and retaining the tooth as a functional unit, this approach renders the tooth nonvital, leading to increased brittleness, loss of proprioceptive feedback, and a higher susceptibility to fracture over the long term. The contemporary paradigm in endodontics has shifted decisively towards pulp preservation and biological repair, a philosophy embodied by vital pulp therapy (VPT). The fundamental objective of VPT is to maintain the health and functionality of the pulp tissue, thereby preserving the tooth's innate biological and defensive capacities. The success of VPT, particularly direct pulp capping, is critically dependent on the biomaterial placed in direct contact with the exposed pulp tissue. This material must be biocompatible, provide a durable seal against bacterial ingress, mitigate inflammation, and, most importantly, stimulate resident pulp progenitor cells to differentiate into odontoblast-like cells that can synthesize a reparative mineralized barrier, known as a dentin bridge. 1,2

For many decades, calcium hydroxide (Ca(OH)2) has been the material of choice and the historical gold standard for direct pulp capping. Its high alkalinity (pH ≈ 12.5) imparts a potent antibacterial effect and induces a mild chemical irritation that is believed to stimulate pulp repair. However, the mechanism of action of Ca(OH)2 involves inducing a superficial liquefaction necrosis at the pulp interface. The reparative dentin that forms beneath this necrotic zone is often porous, discontinuous, and characterized by "tunnel defects," which can serve as pathways for microleakage and eventual treatment failure. Furthermore, Ca(OH)2 is susceptible to dissolution over time, compromising the integrity of the coronal seal. The advent of Mineral Trioxide Aggregate (MTA) and subsequent generations of calcium silicate-based cements marked a significant advancement. These materials demonstrated superior sealing ability, enhanced biocompatibility, and the ability to induce a more homogenous and predictable dentin bridge with

less inflammation compared to Ca(OH)2. Despite their clinical success, these cements are not without limitations, which include difficult handling properties, prolonged setting times, high cost, and the potential for esthetic complications due to tooth discoloration. These subsisting challenges have galvanized research into the development of thirdgeneration "bioactive" materials that do not merely act as passive barriers but actively instruct and guide the biological processes of tissue regeneration. Bioactive glasses (BGs), first conceptualized by Larry Hench, have emerged as a leading class of such materials. These silicate-based amorphous ceramics are defined by their ability to form a strong, direct bond with host tissues. When exposed to physiological fluids, BGs undergo controlled surface dissolution, releasing biologically active ions (primarily Si⁴⁺, Ca²⁺, and PO₄³⁻) into the local microenvironment. This process culminates in the formation of a surface layer of hydroxy-carbonate apatite (HCA), a mineral phase that is chemically and structurally analogous to that of bone and dentin. This HCA layer is osteoconductive, providing a favorable substrate for cell adhesion and growth. More importantly, the released ions, particularly silicic acid (Si(OH)4), act as potent signaling molecules, stimulating the expression of genes associated with osteogenic and odontogenic differentiation in mesenchymal stem cells. 2,3

To amplify the therapeutic efficacy of BGs, a contemporary strategy involves incorporating specific therapeutic ions into the glass network structure. Among various candidates, strontium (Sr2+) has attracted considerable scientific interest musculoskeletal and dental regeneration. Strontium, being in the same group as calcium in the periodic table, exhibits similar chemical behavior and can participate in biological calcification processes. Its therapeutic action is elegantly dual-faceted: it has been robustly demonstrated to stimulate the proliferation and differentiation of osteogenic and odontogenic progenitor cells while concurrently inhibiting the resorptive activity of osteoclasts. In the context of the dentin-pulp complex, strontium ions have been shown to significantly enhance the odontogenic potential of human dental pulp stem cells

(hDPSCs), promoting the formation of mineralized tissue. Furthermore, strontium possesses inherent, dose-dependent antibacterial properties, a crucial attribute for a pulp capping material intended to combat the microbial challenge at the exposure site. While BG powders and cements offer profound biological benefits, their delivery and adaptation to the wound site can be suboptimal. An ideal pulp capping agent should be injectable, allowing for minimally invasive application and ensuring intimate contact with the irregularly shaped pulp wound. Hydrogels, three-dimensional polymeric networks swollen with large amounts of water, represent a superb platform for this purpose. Their soft, hydrated structure closely mimics the native extracellular matrix (ECM), providing an ideal milieu for cell survival, migration, and function. Gelatin, a denatured derivative of collagen, is an exemplary natural polymer for biomedical hydrogels due to its inherent biocompatibility, biodegradability, and the presence of cell-adhesive RGD (arginine-glycine-aspartic acid) Bvfunctionalizing sequences. gelatin with methacryloyl groups, methacrylated gelatin (GelMA) is produced. This modified polymer can be formulated into a precursor solution that remains liquid at physiological temperature but can be rapidly crosslinked into a stable hydrogel upon exposure to light, a process known as photocrosslinking. This provides the clinician with "on-demand" control over the material's placement and solidification. 4-6

This research harnesses the synergistic potential of these advanced material components. We have engineered a novel, injectable, and photocrosslinkable composite hydrogel by dispersing bespoke Sr-BG nanoparticles within a GelMA matrix. This composite design aims to merge the ECM-mimetic and injectable properties of the GelMA hydrogel with the sustained release of therapeutic ions (Sr²⁺, Ca²⁺, Si⁴⁺) from the bioactive glass phase, creating a microenvironment optimized for dentin-pulp regeneration. The novelty of this investigation resides in the rational design and synthesis of a multi-functional, injectable hydrogel specifically engineered for dentin-pulp complex regeneration. Departing from the use of conventional rigid cements, our composite system leverages the

powerful synergy between a photocrosslinkable, cellfriendly gelatin-based hydrogel and ion-releasing Sr-BG nanoparticles. This unique formulation is hypothesized to establish a superior regenerative niche that not only physically protects the pulp but actively orchestrates the fate of resident stem cells, driving them towards an odontogenic lineage. The strategic incorporation of strontium is a key innovative element, conceived to bestow a dual therapeutic advantage of enhanced odontogenesis and intrinsic antibacterial activity, thereby directly confronting the two principal modes of pulp therapy failure: insufficient healing and persistent microbial infection. The overarching aim of this study was to perform a rigorous and comprehensive in vitro and in vivo evaluation of this novel Sr-BG/GelMA hydrogel. The specific objectives were to: Synthesize meticulously characterize the Sr-BG nanoparticles and the final composite hydrogel to establish its physicochemical properties; Quantify the hydrogel's biocompatibility, its capacity to induce odontogenic differentiation in hDPSCs, and its antibacterial efficacy in vitro; Assess its in vivo performance as a direct pulp capping agent in a clinically relevant rat molar model, with a focus on analyzing the quantitative and qualitative aspects of reparative dentin bridge formation and the corresponding pulpal tissue response.

2. Methods

We synthesized strontium-doped bioactive glass nanoparticles of the composition 60SiO_2 –(32-x)CaO– $4\text{P}_2\text{O}_5$ –xSrO (x=8, mol%) using a modified Stöber solgel method. The precursors used were tetraethyl orthosilicate (TEOS, 99.9%, Sigma-Aldrich), calcium nitrate tetrahydrate (Ca(NO₃)₂·4H₂O, 99%, Sigma-Aldrich), triethyl phosphate (TEP, 99.8%, Sigma-Aldrich), and strontium nitrate (Sr(NO₃)₂, 99%, Sigma-Aldrich). In a typical synthesis, we prepared a 1:1 v/v solution of deionized water and absolute ethanol. We added 2 M ammonium hydroxide dropwise to act as a catalyst, adjusting the pH to about 11, while stirring vigorously at room temperature. TEOS was added slowly and allowed to hydrolyze for 30 minutes. Subsequently, we dissolved stoichiometric amounts of

Ca(NO₃)₂·4H₂O, TEP, and Sr(NO₃)₂ in deionized water and added them dropwise to the main solution under continuous stirring. The resulting sol was aged for 72 hours at room temperature to allow for particle formation. The precipitated nanoparticles were collected by centrifugation at 10,000 rpm for 15 minutes, washed three times with deionized water, and twice with absolute ethanol to remove residual reactants. The final product was dried in an oven at 60°C for 24 hours, followed by calcination in a muffle furnace at 700°C for 3 hours to remove nitrates and stabilize the glass structure. A control bioactive glass (BG) without strontium (x=0) was synthesized using the same protocol for comparative purposes. We analyzed the phase composition and crystallinity of the synthesized Sr-BG and BG powders using X-ray Diffraction (XRD) on a Bruker D8 Advance diffractometer with Cu Ka radiation ($\lambda = 1.5406 \text{ Å}$) over a 2θ range of 10° to 70°. The chemical functional groups present in the glass network were identified using Fourier-Transform Infrared Spectroscopy (FTIR) on a PerkinElmer Spectrum Two spectrometer in the range of 400-4000 cm⁻¹, using the KBr pellet method. The morphology, particle size, and elemental composition of the nanoparticles were examined using Scanning Electron Microscopy (SEM) coupled with Energy Dispersive X-ray Spectroscopy (EDS). Samples were sputter-coated with gold and viewed under a JEOL JSM-7600F field emission SEM.

We synthesized Methacrylated Gelatin (GelMA) following a previously established protocol. Briefly, we dissolved 10 g of porcine skin gelatin (Type A, 300 bloom, Sigma-Aldrich) in 100 mL of phosphatebuffered saline (PBS) at 60°C. We added 8 mL of methacrylic anhydride (Sigma-Aldrich) dropwise to the gelatin solution under constant stirring. The reaction was allowed to proceed for 3 hours at 50°C. To stop the reaction, we diluted the solution with warm PBS. The mixture was then dialyzed against deionized water for 7 days using a 12-14 kDa MWCO dialysis to remove unreacted methacrylic membrane anhydride and other byproducts. The purified GelMA solution was lyophilized to obtain a white, porous foam and stored at -20°C until use. We dissolved the lyophilized GelMA in PBS at 10% (w/v) at 37°C. The

photoinitiator, lithium phenyl-2,4,6-trimethylbenzoylphosphinate (LAP, Allevi), was added to a final concentration of 0.5% (w/v). We sterilized the Sr-BG nanoparticles by UV irradiation and then aseptically dispersed them into the GelMA/LAP solution at a concentration of 2% (w/v) using ultrasonication to ensure a homogenous suspension.

This precursor solution was used for all subsequent experiments. We fabricated hydrogel discs by pipetting 100 µL of the precursor solution into cylindrical molds and exposing them to visible blue light (405 nm) for 60 seconds for photocrosslinking. Control hydrogels were fabricated using pure GelMA and GelMA with 2% BG nanoparticles. We determined the swelling ratio of the hydrogels by immersing lyophilized hydrogel discs in PBS at 37°C. At predetermined time points, we removed the samples, blotted off excess surface water, and weighed them. The swelling ratio was calculated as (Wet Weight - Dry Weight) / Dry Weight. We studied the in vitro degradation of the hydrogels by incubating preweighed discs in a PBS solution containing 1.5 U/mL collagenase type II at 37°C. The remaining mass of the hydrogels was measured at various time points after lyophilization. The ion release profile was analyzed by immersing hydrogel discs in Simulated Body Fluid (SBF) at 37°C. At specified time intervals, we collected the SBF solution and measured the concentrations of Si, Ca, P, and Sr ions using Inductively Coupled Plasma-Optical Emission Spectrometry (ICP-OES). We obtained Human Dental Pulp Stem Cells (hDPSCs) from extracted third molars of healthy donors under approved ethical guidelines (IRB #2024-03A) and cultured them in a-MEM medium supplemented with 15% fetal bovine serum (FBS), 100 U/mL penicillin, and 100 µg/mL streptomycin. The cells were maintained at 37°C in a humidified atmosphere of 5% CO₂. We used passages 3-5 for all experiments.

We prepared extracts from the hydrogels according to ISO 10993-5 standards. We incubated hydrogel discs (GelMA, BG/GelMA, Sr-BG/GelMA) in culture medium for 72 hours. We then seeded hDPSCs in a 96-well plate at a density of 5×10³ cells/well. After 24 hours, we replaced the culture medium with the prepared extracts. We quantified cell viability after 1,

3, and 7 days using the MTT (3-(4,5-dimethylthiazol-2-yl)-2,5-diphenyltetrazolium bromide) assay. The absorbance at 570 nm was measured with a microplate reader. For live/dead staining, we cultured hDPSCs on the surface of the hydrogel discs for 3 days and then stained them with calcein-AM (live cells, green) and ethidium homodimer-1 (dead cells, red). We captured images using a fluorescence microscope. We seeded hDPSCs onto the hydrogel discs at a density of 2×10⁴ cells/disc and cultured them in an odontogenic induction medium (standard medium supplemented μg/mL ascorbic acid, 50 10 mM glycerophosphate, and 100 nM dexamethasone). We measured Alkaline Phosphatase (ALP) activity, an early marker of odontogenic differentiation, on days 7 and 14. We lysed the cells and determined ALP activity using a p-nitrophenyl phosphate (pNPP) colorimetric assay kit. We measured the total protein content using a BCA protein assay kit, and normalized ALP activity to the total protein content. We quantified the expression of key odontogenic genes-Dentin Sialophosphoprotein (DSPP), Dentin Matrix Protein 1 (DMP-1), and Runt-related transcription factor 2 (RUNX2)—on day 14 using real-time quantitative polymerase chain reaction (RT-qPCR). We extracted total RNA, reverse transcribed it to cDNA, and amplified it using gene-specific primers. Gene expression levels were normalized to the housekeeping gene GAPDH. We evaluated the antibacterial effect of the hydrogels against Streptococcus mutans (ATCC 25175), a primary cariogenic bacterium. We placed hydrogel discs in 24-well plates and added a bacterial suspension (106 CFU/mL) in Brain Heart Infusion (BHI) broth to each well. The plates were incubated anaerobically at 37°C for 24 hours. We assessed antibacterial activity by measuring the optical density (OD) of the bacterial suspension at 600 nm and by performing a colony-forming unit (CFU) count on BHI agar plates.

All animal procedures were conducted in strict accordance with the guidelines approved by the Institutional Animal Care and Use Committee. We used thirty-six healthy male Wistar rats (8 weeks old, 250-300g). The animals were anesthetized with an intraperitoneal injection of ketamine (80 mg/kg) and

xylazine (10 mg/kg). We prepared Class I cavities on the occlusal surfaces of the maxillary first molars using a sterile 1/4 round bur under constant sterile saline irrigation. We created a standardized pulp exposure of approximately 0.5 mm in diameter at the center of the cavity floor using a sterile endodontic explorer. We achieved hemostasis by gently applying a sterile saline-moistened cotton pellet. The rats were randomly divided into three groups (n=12 per group): Sr-BG/GelMA Group: The pulp exposure was capped with the Sr-BG/GelMA hydrogel precursor, which was then light-cured for 60 seconds; CH Group (Positive Control): The pulp was capped with a calcium hydroxide paste (Dycal, Dentsply Sirona); Untreated Group (Negative Control): The exposed pulp was left untreated. After capping, we restored all cavities with a glass ionomer cement (Fuji IX, GC Corporation). At 4 and 8 weeks post-surgery, we euthanized the animals (n=6 per group per time point). We dissected the maxillae, fixed them in 10% neutral buffered formalin, and decalcified them in 10% EDTA solution for 8 weeks. The decalcified specimens were then dehydrated, embedded in paraffin, and sectioned serially along the mesio-distal plane at a thickness of 5 µm. We stained the sections with Hematoxylin and Eosin (H&E) for general tissue morphology and inflammatory cell infiltration, and with Masson's trichrome for collagen deposition and dentin matrix analysis. Two blinded examiners evaluated the formation of the reparative dentin bridge, pulpal inflammation, and overall tissue organization based on established scoring criteria. Micro-Computed Tomography (Micro-CT) analyzed the maxillae from the 8-week time point by micro-CT (SkyScan 1172) prior to decalcification to quantify the volume and mineral density of the newly formed hard tissue. Scans were performed at a resolution of 10 µm. We reconstructed three-dimensional models and calculated the volume and mineral density of the dentin bridge formed directly beneath the capping material using CTAn software. Statistical Analysis All quantitative data were presented as mean ± standard deviationWe analyzed differences between groups using a one-way analysis of variance (ANOVA) followed by Tukey's posthoc testA p-value of less than 0.05 was considered statistically significant.

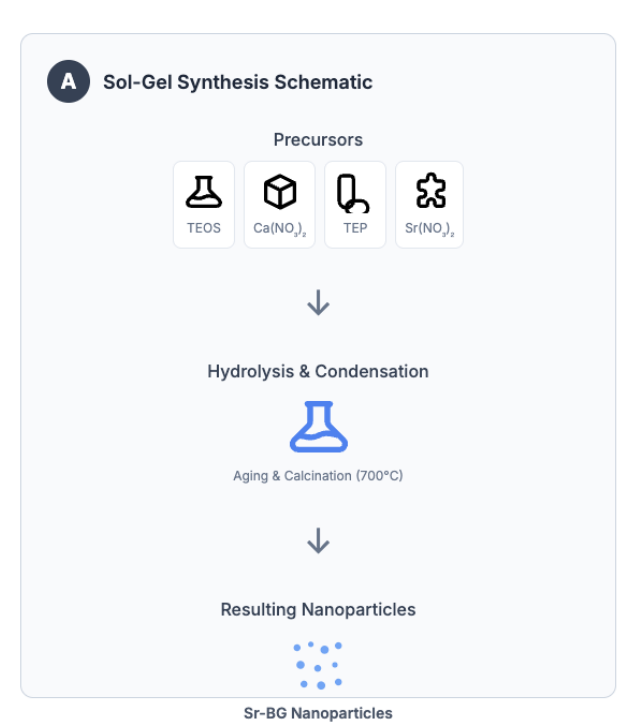
3. Results and discussion

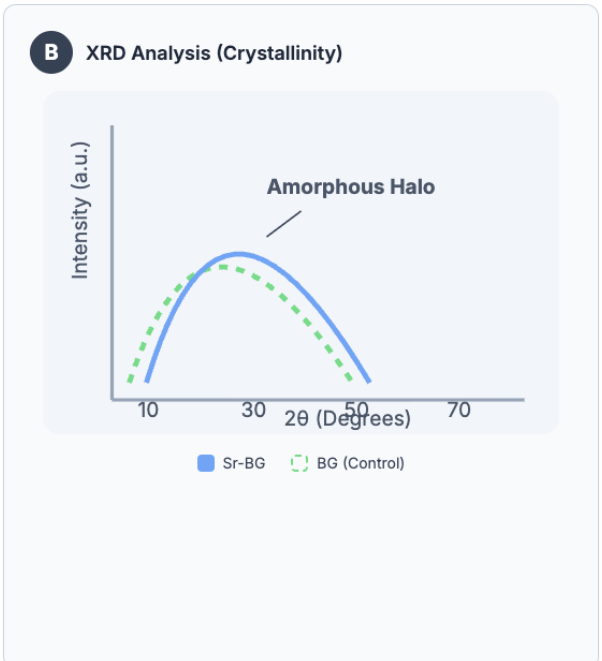
The XRD analysis of both the strontium-free BG and the Sr-BG powders produced patterns with a single, broad diffraction halo centered around 2θ = 20-30°, confirming the successful synthesis of amorphous, non-crystalline materials. The absence of sharp peaks indicated that the calcination process at 700°C was sufficient for stabilization without inducing

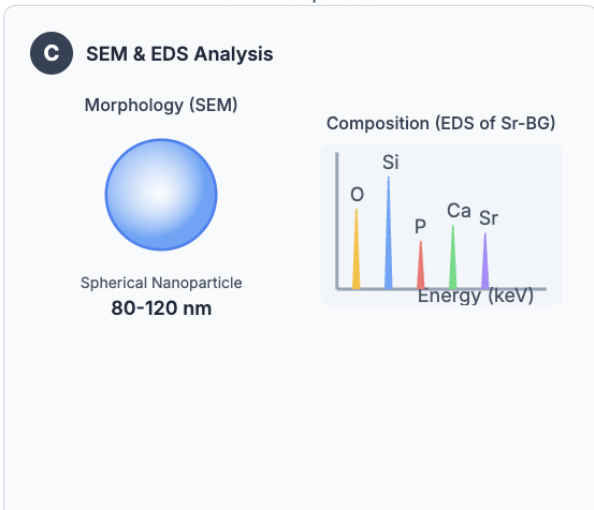
crystallization. SEM imaging revealed that the nanoparticles were predominantly spherical with a smooth surface morphology and a size range of 80-120 nm. The elemental composition was confirmed by EDS, which showed the presence of Si, Ca, P, and O in the BG group, and the additional distinct presence of Sr in the Sr-BG group, verifying the successful incorporation of strontium into the glass network. A summary of nanoparticle characteristics is presented in Figure 1.

Physicochemical Properties of Synthesized Bioactive Glass Nanoparticles

A schematic and graphical summary of the key characterization results for the BG and Sr-BG nanoparticles.







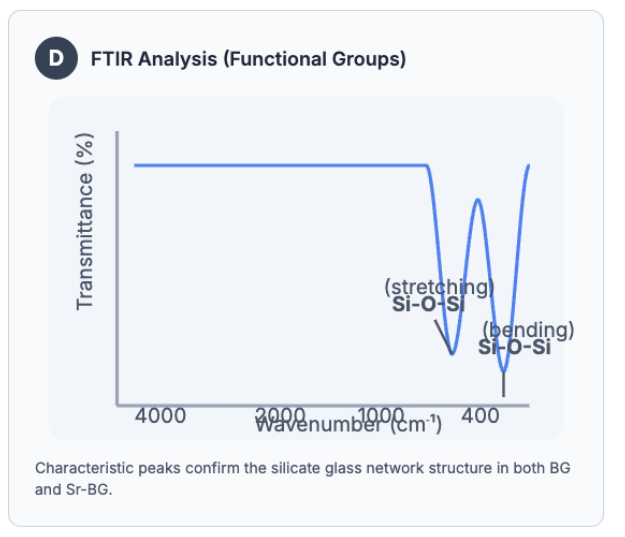


Figure 1. Physicochemical properties of synthesized bioactive glass nanoparticles

We characterized the fabricated hydrogels to assess properties relevant to their application as an injectable scaffold. The swelling behavior, degradation profile, and ion release kinetics are crucial for creating a suitable regenerative environment. The hydrogels demonstrated a high capacity for water absorption, reaching an equilibrium swelling ratio of approximately $850 \pm 45\%$ within 12 hours. The

enzymatic degradation study showed a controlled loss of mass over 28 days, with the Sr-BG/GelMA hydrogel retaining 42.5 \pm 3.1% of its initial weight, suggesting structural stability sufficient to support tissue formation. The cumulative ion release profiles, quantified by ICP-OES, showed a sustained release of all therapeutic ions from the Sr-BG/GelMA hydrogel over 21 days. These results are detailed in Figure 2.

Physical and Chemical Properties of Fabricated Hydrogels

Graphical representation of the swelling, degradation, and ion release profiles of the GelMA-based hydrogels.



Figure 2. Physical and chemical properties of fabricated hydrogels

Biocompatibility and Cell Proliferation evaluated the cytocompatibility of the hydrogels using MTT assays with hDPSCs. All groups demonstrated excellent biocompatibility, with cell viability consistently above 90% relative to the control. Notably, the Sr-BG/GelMA group exhibited a statistically significant increase in cell proliferation at days 3 and 7 compared to both the Pure GelMA and BG/GelMA

groups (p < 0.05). This mitogenic effect suggests that the ions released from the Sr-BG nanoparticles actively stimulated hDPSC proliferation. Live/dead staining visually confirmed these findings, showing a high density of viable, well-spread cells on the surface of all hydrogels. Quantitative results of the MTT assay are shown in Figure 3.

Cell Viability of hDPSCs Cultured with Hydrogel Extracts

A schematic of the MTT assay workflow and quantitative analysis of metabolic activity over 7 days.

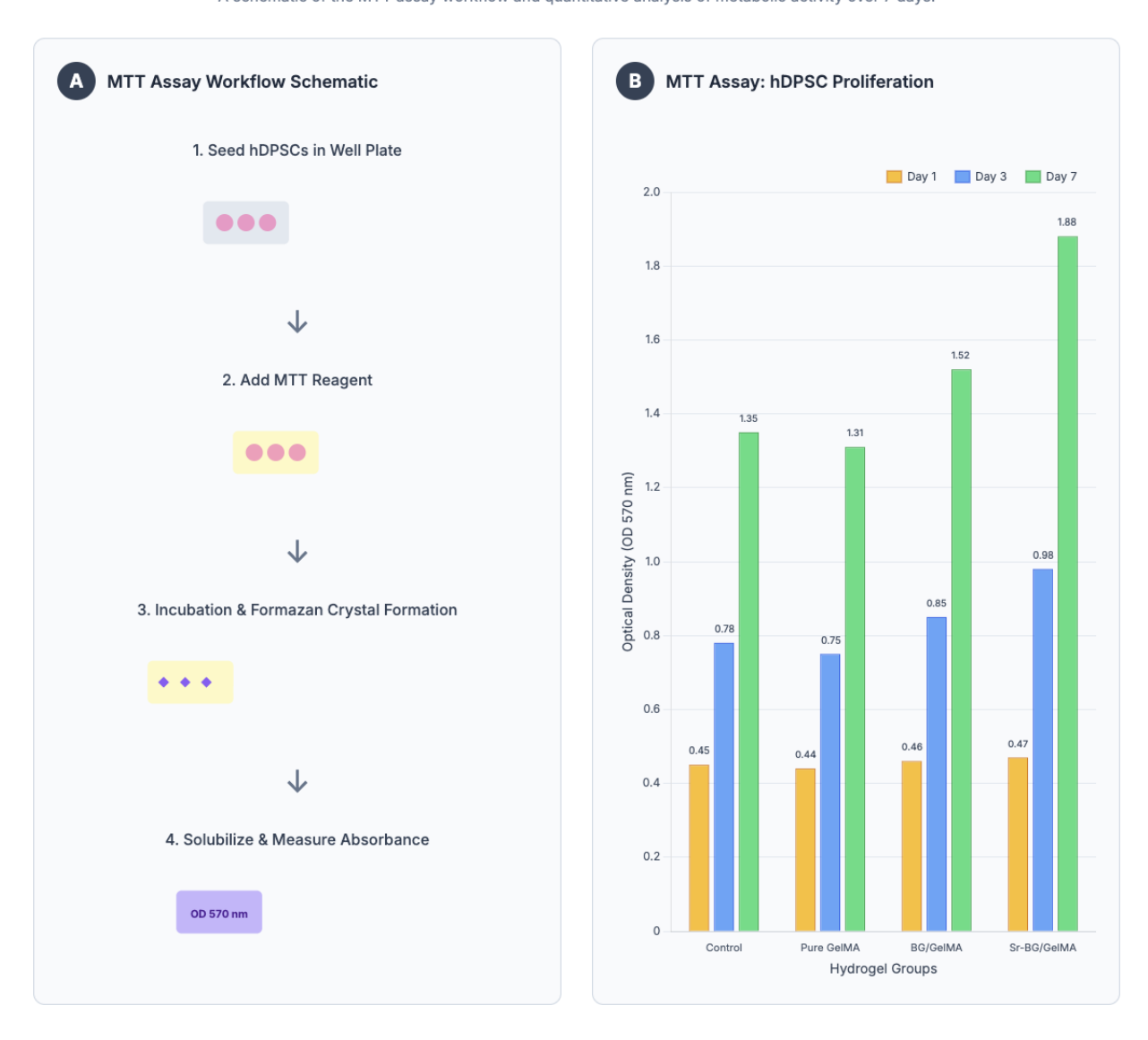


Figure 3. Cell Viability of hDPSCs Cultured with Hydrogel Extracts (MTT Assay)

Odontogenic Differentiation assessed the potential of the hydrogels to induce odontogenic differentiation by measuring ALP activity and gene expression. The Sr-BG/GelMA group showed a significant upregulation of ALP activity at both day 7 and day 14 compared to all other groups (p < 0.05) (Table 4). This indicates an accelerated initiation of mineralization. This finding was further substantiated by RT-qPCR

analysis at day 14. The expression of the master regulator of mineralization, RUNX2, and the key markers of mature odontoblasts, DSPP and DMP-1, was significantly elevated in the Sr-BG/GelMA group. The relative fold increase in DSPP expression was particularly pronounced, highlighting a strong induction towards a secretory odontoblast phenotype (Table 5).

Odontogenic Differentiation of hDPSCs on Hydrogel Scaffolds

A schematic of the differentiation pathway and quantitative analysis of early and late odontogenic markers.



Figure 4. Odontogenic differentiation of hDPSCs on hydrogel scaffolds

Antibacterial Activity quantitatively assessed the antibacterial efficacy against S. mutans. The Sr-BG/GelMA hydrogel demonstrated a potent antibacterial effect, significantly inhibiting bacterial growth as measured by both optical density and CFU

counts. The bacterial viability was reduced by $87.4 \pm 5.6\%$ in the Sr-BG/GelMA group compared to the control. The BG/GelMA group also showed antibacterial activity, but the effect was significantly enhanced by the presence of strontium, in Figure 5.

Antibacterial Activity against S. mutans

A schematic and quantitative analysis of the hydrogels' inhibitory effects on bacterial growth after 24 hours.



Figure 5. Antibacterial activity against S. mutans after 24 hours

Figure 6 provides a detailed, multi-faceted summary of the in vivo outcomes, effectively bridging the procedural methodology with both qualitative histological findings and robust quantitative microcomputed tomography (micro-CT) data. This figure serves as the translational cornerstone of the study, demonstrating the tangible regenerative potential of the Sr-BG/GelMA hydrogel within a clinically relevant animal model. The figure is logically organized into four panels (A, B, C, and D), which collectively narrate the story of the regenerative process from surgical intervention to the final tissue analysis at the 8-week endpoint. Panel A offers a clear and concise schematic of the Surgical Procedure employed in the rat molar model. This panel is crucial for contextualizing the subsequent results, as it illustrates the precise nature of the induced injury and the therapeutic intervention. The four-step process is clearly delineated: (1) a standardized Class I cavity is prepared within the tooth structure, breaching the protective enamel and dentin layers; (2) a deliberate, pinpoint pulp exposure is created, simulating a clinical scenario of deep caries

or trauma; (3) the experimental capping agent, in this case, the Sr-BG/GelMA hydrogel, is applied directly onto the exposed, vital pulp tissue; and (4) a final restoration is placed to seal the cavity from the oral environment.

The accompanying legend provides a clear key for interpreting the various anatomical and material components, ensuring that the reader can fully appreciate the controlled and reproducible nature of the surgical protocol. Panel B presents a powerful, comparative visualization of the Histological Findings at 8 weeks post-surgery. This panel contrasts the healing outcomes of the three experimental groups through simplified, yet scientifically accurate, schematic representations of the dentin-pulp interface. The "Untreated Group" serves as a negative control, and its depiction of widespread pulp necrosis-a complete loss of cellular architecture and vitality-starkly illustrates the consequence of leaving an exposed pulp unprotected. The "CH Group," representing the traditional calcium hydroxide standard-of-care, shows a more favorable but still

suboptimal outcome. The schematic accurately portrays the formation of an "Irregular Bridge," a thin and discontinuous layer of reparative dentin, with an underlying zone of persistent inflammation, depicted as a red circle. This visualizes the known limitations of calcium hydroxide, which often leads to porous, "tunnel-defected" barriers that fail to provide a complete and durable seal. The most striking result is depicted for the "Sr-BG/GelMA Group." The schematic shows the formation of a thick, uniform, and "Complete Bridge" of mineralized tissue, effectively and robustly sealing the site of the original exposure. Crucially, the underlying pulp is labeled as "Healthy Pulp," represented by a calm, light blue color, signifying the absence of significant inflammation and the preservation of normal tissue architecture. This qualitative comparison powerfully suggests that the Sr-BG/GelMA hydrogel not only stimulates hard tissue formation but does so in a manner that is highly biocompatible, fostering a pro-regenerative rather than a pro-inflammatory environment.

Panels C and D transition from qualitative schematics to rigorous, quantitative data derived from high-resolution micro-CT analysis, providing objective validation for the histological observations. Panel C presents a bar chart comparing the Dentin Bridge Volume between the CH Group and the Sr-BG/GelMA Group. The results are unequivocal: the volume of the mineralized bridge formed under the Sr-BG/GelMA hydrogel (0.15 mm³) is nearly double that of the bridge formed under the CH control (0.08 mm³). This statistically significant difference indicates a substantially more robust and extensive regenerative response induced by the experimental hydrogel. It

suggests that the bioactive ions released from the Sr-BG nanoparticles, particularly strontium and silicon, act as potent mitogenic and differentiative signals, recruiting a larger population of progenitor cells and stimulating them to deposit a greater quantity of reparative matrix. Finally, Panel D complements the volume data with an analysis of the Mineral Density of the newly formed tissue. The bar chart reveals that the dentin bridge in the Sr-BG/GelMA group (1.28 g/cm³) is significantly denser than that in the CH group (0.95 g/cm³).

This is a critically important finding, as it speaks to the quality of the regenerated tissue, not just the quantity. A higher mineral density implies a more organized, compact, and well-mineralized structure, which is likely to provide a superior long-term seal against microleakage and bacterial invasion. This result suggests that the sustained release of calcium, phosphate, and strontium ions from the hydrogel creates an ionically enriched microenvironment that promotes more efficient and complete mineralization of the deposited collagen matrix, leading to the formation of a hard tissue barrier that more closely resembles the properties of natural dentin. Figure 6 masterfully integrates procedural context, qualitative tissue analysis, and quantitative mineral analysis to build a compelling case for the superior in vivo efficacy of the novel Sr-BG/GelMA hydrogel. It visually and numerically demonstrates that the material not only surpasses the traditional standard-of-care but also promotes a healing outcome characterized by true regeneration—the formation of a substantial, highquality, and well-integrated dentin bridge over a healthy, vital pulp.

In Vivo Regenerative Efficacy

Schematic and quantitative analysis of dentin-pulp complex regeneration in the rat molar model at 8 weeks.

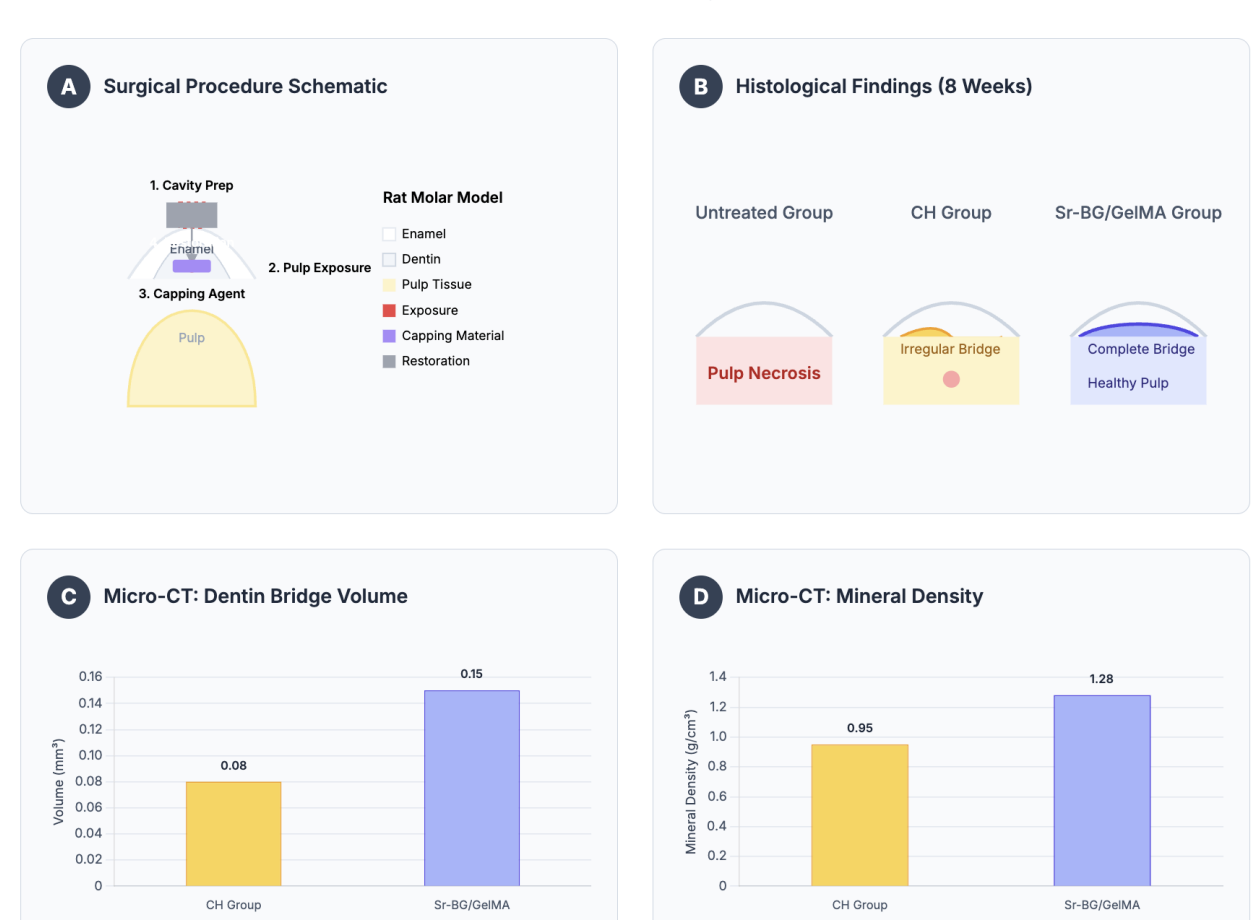


Figure 6. In vivo regenerative efficacy

The successful regeneration of the dentin-pulp complex following injury represents a pinnacle of regenerative dentistry, aiming to restore not just form but full biological function. The findings of this investigation provide compelling evidence that the rationally designed Sr-BG/GelMA hydrogel is a potent bioactive material capable of orchestrating a robust regenerative response. The foundation of the hydrogel's success lies in its meticulously engineered composition. The choice of GelMA as the scaffold backbone was strategic. As a derivative of collagen, the primary organic component of the dentin-pulp ECM, GelMA provides an inherently biomimetic and cellfriendly environment. Its photocrosslinkable nature confers a critical translational advantage, allowing it to be applied as a liquid that conforms perfectly to the irregular geometry of the pulp wound before being rapidly solidified in situ. This ensures intimate

material-tissue contact, which is essential for both effective sealing and biological signaling. The observed controlled degradation profile is equally important; the scaffold persists long enough to provide mechanical support and guide initial tissue formation but gradually resorbs to allow for complete replacement by native, newly synthesized ECM.⁷⁻¹⁰

The true bio-instructive capability of the hydrogel, however, is derived from the Sr-BG nanoparticles. The sol-gel synthesis method we used yielded amorphous, nanosized particles, a morphology that maximizes surface area and, consequently, enhances their reactivity and ion exchange capacity. The sustained release of Ca²⁺, PO₄³⁻, Si⁴⁺ (as Si(OH)₄), and Sr²⁺ ions transforms the local wound microenvironment from a site of injury into a pro-regenerative niche. The released Ca²⁺ and PO₄³⁻ ions increase the local supersaturation, thermodynamically favoring the

precipitation of calcium phosphate phases and providing the mineral building blocks for the new dentin bridge. This process is further supported by the well-documented ability of silicic acid to nucleate apatite formation. The most profound biological effects were linked to the release of silicon and strontium ions. Silicic acid is not merely a structural component; it is a potent signaling molecule. It has been shown to stimulate the autocrine production of growth factors by progenitor cells and to directly upregulate the transcription of genes essential for ECM synthesis, most notably type I collagen, the principal organic component of the dentin matrix. This explains, in part, the robust matrix deposition we observed in the in vivo model. The incorporation of strontium was the key innovative element, and its impact was unequivocally demonstrated in the results. The significant mitogenic effect on hDPSCs we observed in vitro is consistent with reports of strontium's ability to activate signaling pathways, such as the MAPK/ERK pathway, which are known to promote cell cycle progression and proliferation. This initial expansion of the local progenitor cell pool is a critical first step in mounting an effective regenerative response. Even more striking was strontium's potent induction of odontogenic differentiation. The dramatic upregulation of RUNX2, the master transcription factor for hard tissue formation, followed by the robust expression of DSPP DMP-1, terminal markers odontoblasts, confirms that strontium effectively directs the fate of hDPSCs towards a mineralizing lineage.11-13

The proposed mechanism for this effect involves the interaction of Sr2+ ions with the calcium-sensing receptor (CaSR) present on the surface of hDPSCs. As a divalent cation with an ionic radius similar to calcium, strontium can act as a CaSR agonist, triggering downstream intracellular signaling cascades, including the activation of phospholipase C and subsequent pathways that converge on the nucleus to activate odontogenic gene transcription programs. The near eight-fold increase in DSPP expression is particularly significant, as DSPP is a crucial non-collagenous protein that regulates the nucleation and growth of hydroxyapatite crystals

during dentinogenesis. This potent stimulation of a specific, mature odontoblast phenotype is directly responsible for the superior quality of the dentin bridge formed in vivo-a structure that was not only thicker but also histologically more organized and tubular, resembling native reactionary dentin rather than the atubular, scar-like tissue often seen with traditional materials. From a pathophysiological standpoint, the hydrogel's properties directly counter the primary challenges of pulp healing. Following pulp exposure, the tissue is immediately confronted with bacterial contamination and an ensuing inflammatory response. If uncontrolled, inflammation can become destructive, leading to extensive tissue damage and necrosis. The Sr-BG/GelMA hydrogel addresses this in two ways. First, its inherent antibacterial activity, significantly augmented by strontium, helps to control the microbial burden at the wound site. The mechanism is likely multifactorial, involving the creation of an alkaline pH, the generation of osmotic stress, and potentially direct interference of Sr2+ with bacterial enzymatic processes. By reducing the bacterial challenge, the hydrogel mitigates a primary driver of persistent inflammation. 14-17

Second, the bioactive ions themselves may have an immunomodulatory effect. Recent studies suggest that ions like silicon and strontium can polarize macrophage responses away from a pro-inflammatory (M1) phenotype towards a pro-regenerative (M2) phenotype. An M2-dominant environment is characterized by the secretion of anti-inflammatory cytokines (like IL-10) and growth factors (like TGF-β and VEGF) that promote tissue repair and angiogenesis. The remarkably quiescent and healthy appearance of the pulp tissue beneath the Sr-BG/GelMA hydrogel in our in vivo model, devoid of the significant inflammatory infiltrate seen in the CH group, strongly suggests that the material not only stimulated regeneration but also actively fostered a pro-healing, anti-inflammatory milieu. The in vivo results represent a culmination of these favorable in vitro properties. The direct comparison with calcium hydroxide, the long-standing clinical benchmark, was particularly revealing. While Ca(OH)2 did induce a mineralized barrier, its mechanism, which relies on

inducing necrosis, resulted in a qualitatively inferior structure. The tunnel defects and inflammation we observed are well-known limitations that compromise the long-term seal and pulp health. In contrast, the Sr-BG/GelMA hydrogel promoted healing through a process of true regeneration. It appeared to recruit and stimulate endogenous stem cells to differentiate and deposit a well-organized, dense dentin bridge without an intervening necrotic layer. The quantitative micro-CT data provided objective validation of this superiority, confirming that the bridge formed under the hydrogel was significantly larger and more densely mineralized. This suggests a more rapid and complete healing process, leading to a more robust and protective barrier that can effectively and permanently isolate the pulp from the oral environment. This work successfully demonstrates that by integrating advanced material science with a deep understanding of pulp biology, it is possible to create biomaterials that move beyond simple repair and truly embrace the potential of endogenous tissue regeneration. 18-20

4. Conclusion

Within the scope of this investigation, it was unequivocally concluded that the novel, injectable Sr-BG/GelMA hydrogel represents a highly effective and advanced biomaterial for the regeneration of the dentin-pulp complex. Through the strategic combination of the biomimetic scaffold properties of GelMA and the multifaceted therapeutic bioactivity imparted by the sustained release of ions from strontium-doped bioactive glass, this hydrogel successfully orchestrated the formation of a thick, continuous, and highly organized reparative dentin bridge in an in vivo pulp capping model. The in vitro findings confirmed its excellent biocompatibility, to stimulate odontogenic potent capacity differentiation in human dental pulp stem cells, and significant antibacterial efficacy. By directly addressing the key biological and pathological challenges of pulp injury, this advanced biomaterial demonstrates a clear superiority over traditional pulp capping agents and holds substantial promise for enhancing the predictability, quality, and long-term success of vital pulp therapy in clinical practice.

5. References

- Souza AP, Neves JG, Navarro da Rocha D, Lopes CC, Moraes ÂM, Correr-Sobrinho L, et al. Chitosan/Xanthan/Hydroxyapatitegraphene oxide porous scaffold associated with mesenchymal stem cells for dentin-pulp complex regeneration. J Biomater Appl. 2023;37(9):1605-16.
- Hammouda DA, Mansour AM, Saeed MA, Zaher AR, Grawish ME. Stem cell-derived exosomes for dentin-pulp complex regeneration: a mini-review. Restor Dent Endod. 2023;48(2):e20.
- Spagnuolo G, De Luca I, Iaculli F, Barbato E, Valletta A, Calarco A, et al. Regeneration of dentin-pulp complex: Effect of calcium-based materials on hDPSCs differentiation and gene expression. Dent Mater. 2023;39(5):485–91.
- 4. Luo N, Deng Y-W, Wen J, Xu X-C, Jiang R-X, Zhan J-Y, et al. Wnt3a-loaded hydroxyapatite nanowire@mesoporous silica core-shell nanocomposite promotes the regeneration of dentin-pulp complex via angiogenesis, oxidative stress resistance, and odontogenic induction of stem cells. Adv Healthc Mater. 2023;12(22):e2300229.
- Li Y, Wu M, Xing X, Li X, Shi C. Effect of Wnt10a/β-catenin signaling pathway on promoting the repair of different types of dentin-pulp injury. In Vitro Cell Dev Biol Anim. 2023;59(7):486-504.
- Amir M, Jeevithan L, Barkat M, Fatima SH, Khan M, Israr S, et al. Advances in regenerative dentistry: A systematic review of harnessing Wnt/β-Catenin in dentin-pulp regeneration. Cells. 2024;13(13):1153.
- 7. Han S, Wang L, Peng X, Wang J, Ou Y, Tao Y, et al. Amelogenin-inspired autoadaptive peptide in a caries microenvironment facilitates long-term protection of the dentinpulp complex. ACS Appl Mater Interfaces. 2024;16(31):41518–33.
- 8. Abbass MMS, El-Rashidy AA, Sadek KM, Moshy SE, Radwan IA, Rady D, et al. Hydrogels and dentin-pulp complex

- regeneration: From the benchtop to clinical translation. Polymers (Basel). 2020;12(12):2935.
- 9. Xia K, Chen Z, Chen J, Xu H, Xu Y, Yang T, et al. RGD- and VEGF-mimetic peptide Epitope-functionalized self-assembling peptide hydrogels promote dentin-pulp complex regeneration. Int J Nanomedicine. 2020;15:6631–47.
- 10. Bakhtiar H, Mousavi MR, Rajabi S, Pezeshki-Modaress M, Ayati A, Ashoori A, et al. Fabrication and characterization of a novel injectable human amniotic membrane hydrogel for dentin-pulp complex regeneration. Dent Mater. 2023;39(8):718.
- Smith AJ, Duncan HF, Diogenes A, Simon S, Cooper PR. Exploiting the bioactive properties of the dentin-pulp complex in regenerative endodontics. J Endod. 2016;42(1):47–56.
- 12. Shrestha S, Kishen A. Bioactive molecule delivery systems for dentin-pulp tissue engineering. J Endod. 2017;43(5):733–44.
- 13. Dalmolin AC, Acevedo LFA, Campos LA, Dechandt ICJ, Serbena FC, Zanotto ED, et al. Effect of bioactive glasses used as dentin desensitizers on the dentin-pulp complex in rats. Dent Mater J. 2022;41(6):874–81.
- 14. Jikia T, Chipashvili N. Tissue engineering scaffolds for dentin-pulp complex regeneration. Georgian Biomed News. 2024.
- 15. Edranov SS, Kalinichenko SG, Matveeva NY, Kovaleva IV. Morphogenetic and growth factors in damaging to the dentin-pulp complex and periodontium. Pac Med J. 2024;(1):11-6.
- 16. Mitronin AV, Ostanina DA, Alimukhamedova SS, Fulova AM. Changes in the dentin-pulp complex of teeth through the prism of CBCTstudies: A retrospective analysis. Èndodontiâ Today. 2025.
- 17. Osman M, Sharmin Z, Suchy S, Gao F, Kaminski A, Mitchell JC, et al. Bioinspired smart dentin ECM-chitosan hydrogels for dentin-pulp complex regeneration. J Dent. 2025;159(105811):105811.

- 18. de Souza Araújo IJ, Perkins RS, Zhang W, Krum SA, Huang GT-J. Canonical and noncanonical WNT-loaded hydrogel for dentin-pulp regeneration. J Dent Res. 2025; 220345251357588.
- Sismanoglu S, Işık V, Ercal P. Regenerative dentistry: Applications of bioactive materials in dentin-pulp complex. Adv Exp Med Biol. 2025.
- 20. Mandakhbayar N, El-Fiqi A, Lee J-H, Kim H-W. Evaluation of strontium-doped nanobioactive glass cement for dentin-pulp complex regeneration therapy. ACS Biomater Sci Eng. 2019;5(11):6117–26.